HHS Public Access

Author manuscript

*Biochem J.* Author manuscript; available in PMC 2018 February 13.

Published in final edited form as:

*Biochem J.* 2014 November 15; 464(1): 73–84. doi:10.1042/BJ20140766.

# TRPC1 contributes to the $Ca^{2+}$ -dependent regulation of adenylate cyclases

**Debbie Willoughby**[*], **Hwei Ling Ong**[†], **Lorena Brito De Souza**[†], **Sebastian Wachten**[*], **Indu S. Ambudkar**[†], and **Dermot M. F. Cooper**[*,1]

[*]Department of Pharmacology, University of Cambridge, Tennis Court Road, Cambridge CB2 1PD, U.K

[†]Secretory Physiology Section, Molecular Physiology and Therapeutics Branch, National Institute of Dental and Craniofacial Research, National Institutes of Health, Bethesda, MD 20892-1190, U.S.A

## Abstract

SOCE (store-operated $Ca^{2+}$ entry) is mediated via specific plasma membrane channels in response to ER (endoplasmic reticulum) $Ca^{2+}$ store depletion. This route of $Ca^{2+}$ entry is central to the dynamic interplay between $Ca^{2+}$ and cAMP signalling in regulating the activity of $Ca^{2+}$ -sensitive adenylate cyclase isoforms (AC1, AC5, AC6 and AC8). Two proteins have been identified as key components of SOCE: STIM1 (stromal interaction molecule 1), which senses ER $Ca^{2+}$ store content and translocates to the plasma membrane upon store depletion, where it then activates Orai1, the pore-forming component of the CRAC ($Ca^{2+}$ release-activated $Ca^{2+}$) channel. Previous studies reported that co-expression of STIM1 and Orai1 in HEK-293 (human embryonic kidney 293) cells enhances $Ca^{2+}$ -stimulated AC8 activity and that AC8 and Orai1 directly interact to enhance this regulation. Nonetheless, the additional involvement of TRPC (transient receptor potential canonical) channels in SOCE has also been proposed. In the present study, we evaluate the contribution of TRPC1 to SOCE-mediated regulation of $Ca^{2+}$ -sensitive ACs in HEK-293 cells stably expressing AC8 (HEK-AC8) and HSG (human submandibular gland) cells expressing an endogenous $Ca^{2+}$ -inhibited AC6. We demonstrate a role for TRPC1 as an integral component of SOCE, alongside STIM1 and Orai1, in regulating $Ca^{2+}$ fluxes within AC microdomains and influencing cAMP production.

### Keywords

adenylate cyclase; Orai1; STIM1; store-operated $Ca^{2+}$ -entry; TRPC1

[1]To whom correspondence should be addressed (dmfc2@cam.ac.uk).

**AUTHOR CONTRIBUTION**

Debbie Willoughby, Hwei Ling Ong, Lorena Brito De Souza and Sebastian Wachten planned and performed the experiments and data analysis. Debbie Willoughby, Indu Ambudkar and Dermot Cooper analysed the data and wrote the paper.

## INTRODUCTION

Several AC (adenylate cyclase) isoforms respond to intracellular $Ca^{2+}$ changes with acute changes in cAMP synthesis [1]. Of the nine membrane-bound AC isoforms, AC1 and AC8 are stimulated by a well-defined interaction with $Ca^{2+}$ /CaM (calmodulin) [2–6], whereas AC5 and AC6 are directly inhibited by $Ca^{2+}$ [7,8]. Thus the $Ca^{2+}$ -sensitive ACs are principal sites for cross-talk, integrating the activities of two major signalling pathways. The regulation of cAMP production by $Ca^{2+}$ is selective for specific intracellular $Ca^{2+}$ events, brought about by the residence of the ACs in highly organized cellular microdomains [1,9]. In particular, the $Ca^{2+}$ -sensitive ACs are remarkably selective for regulation by SOCE (store-operated $Ca^{2+}$ entry) following depletion of ER (endoplasmic reticulum) $Ca^{2+}$ stores [1,10]. A limited sensitivity of the ACs to $IP_3$ (inositol 1,4,5-trisphosphate)-mediated $Ca^{2+}$ release in the absence of external $Ca^{2+}$ has been observed in subpopulations of cells [11,12], but $Ca^{2+}$ entry mediated via ionophore-, arachidonic acid- or OAG (1-oleyl-2-acetyl-*sn*-glycerol)-dependent pathways is ineffective with respect to AC regulation [10,13,14]. Selectivity for SOCE is also seen in excitable cells, with modest SOCE events regulating AC activity to a comparable degree as the more robust $Ca^{2+}$ signals arising from VGCCs (voltage-gated $Ca^{2+}$ channels) [15].

The identification of two major molecular components of SOCE has provided great insight into the precise mechanisms underlying cellular $Ca^{2+}$ entry linked to ER store depletion. STIM1 (stromal interaction molecule 1) acts as a sensor of ER $Ca^{2+}$ content by possessing at the N-terminus a low-affinity EF hand that resides within the lumen of the ER [16,17]. In response to store depletion, STIM1 forms clusters at the ER–plasma membrane junctions [18,19]. A second protein, Orai1, has been identified as the pore-forming subunit of CRAC ($Ca^{2+}$ release-activated $Ca^{2+}$) channels, which were first identified in mast cells and lymphocytes [20–22]. CRAC channels are generated by the assembly of Orai1 tetramers [23–25]. The relocalization and clustering of STIM1 triggers the recruitment of Orai1 into puncta, with subsequent STIM1-mediated gating of the Orai1 channel [26]. We have shown recently that direct binding between the N-termini of Orai1 and AC8 ensures a dynamic and co-ordinated interaction between SOCE and cAMP signalling in discrete AC microdomains [9]. However, it remains to be seen whether other AC isoforms can bind Orai1 or whether other potential SOCE channel components participate in the interaction to promote interplay between $Ca^{2+}$ and cAMP signalling.

Before the identification of Orai1 as the pore-forming subunit of SOC channels, the TRPC (transient receptor potential canonical) channels were leading candidates for this role [27]. There is sufficient evidence that endogenous TRPC1 is involved in SOCE in several cell types [28]. Although a number of studies contest a role for TRPC1 as components of SOCE channels [29–31], studies from several laboratories have shown that TRPC1 forms a complex with STIM1 and Orai1 and, more importantly, that TRPC1 is dependent on both proteins for activation in response to $Ca^{2+}$ -store depletion [32–35]. Gating of TRPC1 by STIM1 is reported to occur via a region distinct from that involved in the gating of Orai1. Electrostatic interactions between the polybasic C-terminal $Lys^{684}$–$Lys^{685}$ residues of STIM1 and conserved aspartate residues ($Asp^{639}$–$Asp^{640}$) in TRPC1 have been demonstrated to be involved in gating of TRPC1 [36]. Furthermore, the functional

interaction between TRPC1 and STIM1 is seemingly confined to lipid raft regions of the membrane [37,38]. Significantly, TRPC1 activation by STIM1 depends on functional Orai1 channels [32,36]. We proposed recently that Orai1 regulates plasma membrane recruitment of TRPC1 where it is subsequently gated by STIM1. The present study established that Orai1–STIM1 and TRPC1–STIM1 function as distinct CRAC and SOCE channels respectively, that reside in close proximity to each other. Nevertheless, the two channels appear to contribute to distinct downstream functions. We showed that Orai1-CRAC channels preferentially regulate NFAT (nuclear factor of activated T-cells) activation, suggesting a very close coupling between Orai1 and regulation of NFAT [39]. In the present study, we investigated another downstream target, AC, which is also regulated by Orai1-mediated $Ca^{2+}$ entry. Based on the observation that TRPC1 and Orai1 are localized in close proximity to each other, we assessed the possible contribution of TRPC1 to $Ca^{2+}$ -microdomains involved in the regulation of ACs.

In the present study, we have used genetically encoded fluorescent sensors of $Ca^{2+}$ and cAMP to examine the contribution of TRPC1 to SOCE-mediated regulation of two different AC isoforms. We compared data from HEK-293 (human embryonic kidney 293) cells stably expressing $Ca^{2+}$ -stimulated AC8 (referred to as HEK-AC8) and HSG (human submandibular gland) cells expressing an endogenous $Ca^{2+}$ -inhibited AC6. AC-targeted versions of the $Ca^{2+}$ and cAMP sensors were used for high-resolution measurements of $Ca^{2+}$ and cAMP changes taking place within the ‘AC8 microdomain’. This was combined with RNAi techniques to examine the dependence of TRPC1 action on Orai1 expression. We demonstrate that TRPC1 is an important component of SOCE and, acting alongside STIM1 and Orai1, it contributes to $Ca^{2+}$ fluxes within the AC microdomain that control local cAMP production.

## EXPERIMENTAL

### Cell culture and transfection

HSG and HEK-293 cells were grown in MEM (minimum essential medium) supplemented with 10% (v/v) FBS, 50 units/ml penicillin, 50 μg/ml streptomycin and 2 mM L-glutamine and maintained at 37°C in 95%air and 5%$CO_2$. Cells were plated on to either 100-mm-diameter dishes or 25 mm poly-L-lysine coated coverslips. Lipofectamine 2000 (Invitrogen) was used for DNA and shRNA transfections, whereas Lipofectamine RNAiMAX (Invitrogen) was used for siRNA transfection, following the manufacturer’s instructions. For siRNA experiments, smartpool oligonucleotides directed against Orai1 (catalogue number L-014998-00-0005, Dharmacon, Thermo Scientific), or scrambled siRNA control oligonucleotides (catalogue number D-001810-10-05) were transfected at a final concentration of 25 nM. Sequences for the shRNA targeting human TRPC1 have been described previously [34]. Cells were used 48–72 h post-transfection.

To produce stably expressing HEK-AC8 cells, wild-type HEK-293 cells were plated on to 100-mm-diameter dishes at ~60% confluency 1 day before transfection with 2 μg of rat AC8 using the Lipofectamine 2000 transfection method. Then, 2 days later, the culture medium was replaced with fresh medium containing 800 μg/ml G-418 disulfate (Formedium) to select transfected cells. After selection, cells were maintained in medium containing 400

μg/ml G-418. Stable AC8-expressing HEK-293 cells were established from ~2 weeks following transfection.

### Fura 2 $Ca^{2+}$ measurements

Cells were plated on to 25 mm poly-L-lysine-coated coverslips 24 h before loading with 4 μM fura 2/AM (fura 2 acetoxymethyl ester) and 0.02% Pluronic F-127 (Molecular Probes) for 40 min at room temperature in standard Hepes-buffered saline containing: 140 mM NaCl, 4 mM KCl, 1 mM $CaCl_2$, 0.2 mM $MgCl_2$, 11 mM D-glucose and 10 mM Hepes, pH 7.4. After loading, cells were washed several times and imaged using a CoolSNAP-HQ CCD (charge-coupled-device) camera (Photometrics) and monochromator system (Cairn Research) attached to a Nikon TMD microscope (×40 objective). Emission images (D510/80M) at 340 nm and 380 nm excitation were collected at 1 Hz using MetaFluor software (Molecular Devices). For zero calcium buffer, 1 mM $CaCl_2$ was omitted and replaced by 100 μM EGTA.

### GCaMP2 and GCaMP2-AC8 measurements

$Ca^{2+}$ measurements using GCaMP2-based constructs were performed using an iXon EMCCD camera (Andor). Cells were excited at 488 nm using a monochromator (Cairn Research) and ET-GFP filter set (with 495DC and 525/50 emitter) (Chroma) attached to a Nikon eclipse TE2000-Smicroscope (×40 objective). Emission images were collected every 3–5 s (250–300 ms integration time), background subtracted and analysed using MetaMorph imaging software (Molecular Devices). Data were normalized to the maximal GCaMP2 signal seen upon the addition of 10 mM $Ca^{2+}$ plus 5 μM ionomycin.

### Epac2-camps and Epac2-camps-AC8 FRET measurements

Epac2-camps- or Epac2-camps-AC8-expressing HEK-293 cells were imaged using an Andor iXon EMCCD camera and an Optosplit (505DC) to separate CFP (470 nm) and YFP (535 nm) emission images (Cairn Research). For dual emission ratio imaging, cells were excited at 435 nm using a monochromator (Cairn Research) and 51017 filter set (Chroma) attached to a Nikon eclipse TE2000-S microscope (×40 objective). Emission images at 470 nm and 535 nm were collected every 3–5 s (250 ms integration time) and analysed using MetaMorph imaging software (Molecular Devices). Cells in which the CFP and YFP fluorescence intensity was less than twice the background signal were excluded, as were cells with excessive expression of the fluorescent probe [11]. Single cell FRET data are plotted as changes in background subtracted 470 nm (CFP) compared with 535 nm (YFP) emission ratio normalized to the maximal FRET change ($\Delta F/F_{max}$) seen during the addition of a cocktail to saturate the FRET sensor [containing 100 μM IBMX (isobutylmethylxanthine), 10 μM isoproterenol and 10 μM Fsk (forskolin)].

### TIRF (total internal reflection fluorescence) microscopy

An Olympus IX81 motorized inverted microscope (Olympus) was used as described previously [34] using 447, 514 and 568 nm lasers for excitation of CFP, YFP and mCherry respectively, a TIRF-optimized Olympus Plan APO ×60 [1.45 NA (numerical aperture)] oil immersion objective and Lambda 10-3 filter wheel (Sutter Instruments) containing 480/40m,

525/50m and 605/52m band pass filters for emission. There is negligible bleed-through associated with these filters at the wavelengths used. Images were collected using a QImaging Rolera EM-C2 camera and MetaMorph imaging software (Molecular Devices). MetaMorph was also used to measure line scans and the fluorescence intensities of selected ROIs (regions of interest) before and after cell stimulation with Tg (thapsigargin). These values taken from TIRF images were then plotted and analysed using Origin 8 software (OriginLab). Experimental values are expressed as means±S.E.M., with statistical comparisons made using the Student's *t* test. Differences in the mean values were considered to be significant at $P < 0.01$.

### RT-PCR (reverse transcription–PCR)

Total RNA was prepared from HSG cells using the RNeasy Mini Kit (Qiagen). Total RNA (2 μg) was transcribed into cDNA using SuperScript II Reverse Transcriptase (Invitrogen). DNA fragments were amplified from HSG cDNA using the KOD Hot-Start DNA polymerase (Novagen). Amplified fragments were separated on a 0.85% agarose gel and visualized with SafeView nucleic acid stain (NBS Biologicals).

### Western blotting

HSG and HEK-293 cells were washed with PBS and lysed in RIPA protein extraction buffer [50 mM Tris/HCl, 150 mM NaCl, 0.1% SDS, 0.5%sodium deoxycholate, 1%(v/v) Triton X-100, 2 mM EDTA and 1 mM DTT, pH 7.4] supplemented with Complete™ protease inhibitor cocktail tablets (Roche Diagnostics). Cell lysates were then centrifuged at 16500 ***g*** for 30 min at 4°C and the supernatant was collected. Proteins were resolved using NuPAGE (4–12% gels) (Invitrogen), followed by Western blotting with the anti-TRPC1 antibody (1:00 dilution) [34].

### Statistical analysis

Unless stated otherwise, data were analysed by one-way ANOVA followed by Bonferroni or Tukey multiple comparisons tests, depending on whether one or more than one pair of data were being investigated (GraphPad Prism). Data are presented as means±S.E.M., with significance set at $P < 0.05$.

## RESULTS

### SOCE-induced AC8 activity is sensitive to TRPC1 expression levels

To establish whether TRPC1 contributes to the SOCE signal that regulates AC8 activity, single cell imaging experiments were performed to monitor the $Ca^{2+}$ and cAMP changes seen when TRPC1 expression levels were altered. SOCE was induced experimentally in HEK-AC8 cells expressing either the $Ca^{2+}$ sensor GCaMP2 or cAMP sensor, Epac2-camps. Successful use of these sensors to monitor $Ca^{2+}$ and cAMP changes during SOCE events in HEK-AC8 cells has been demonstrated previously [12]. Under control conditions, the addition of 1 mM external $Ca^{2+}$ to HEK-AC8 cells pre-treated with a SERCA (sarcoplasmic/endoplasmic reticulum $Ca^{2+}$ -ATPase) pump inhibitor (200 nM Tg to passively deplete ER $Ca^{2+}$ stores) was accompanied by a sustained increase in cytosolic $Ca^{2+}$ levels (Figure 1A) and a parallel rise in cAMP signal (Figure 1B). (The rise in cAMP is absolutely dependent

on the expression of AC8, as described previously [4,11]). Addition of 100 μM 2APB (2-aminoethoxydiphenyl borate), an inhibitor of SOCE [40], blocked both $Ca^{2+}$ entry and the accompanying rise in cAMP, confirming a dependence of AC8 activity on SOCE (Figures 1A and 1B). In a similar series of experiments the addition of 0.5 mM $Ca^{2+}$ to Tg-pre-treated HEK-AC8 cells overexpressing HA (haemagglutinin)–STIM1 plus Myc–Orai1 resulted in enhanced $Ca^{2+}$ entry (Figures 1C and 1D; $P < 0.01$) and larger $Ca^{2+}$ -dependent cAMP production (Figure 1E and 1F; $P < 0.01$) compared with controls. These data were consistent with previous work from our group linking STIM1 and Orai1 expression to enhanced AC8 activity [41]. In the present study, expression of HA–TRPC1 alongside HA–STIM1 and Myc–Orai1 enhanced both the $Ca^{2+}$ and cAMP signal associated with SOCE (Figures 1C–1F; $P < 0.05$ compared with HA–STIM1 and Myc–Orai1 expression). In contrast, overexpression of TRPC1 alone resulted in a small reduction in $Ca^{2+}$ entry and no significant change in the degree of AC8 activity when compared with control HEK-AC8 cells (Figure 1C–1F). An earlier study [42] reported that overexpression of Orai1 reduced endogenous SOCE, and attributed this to an imbalance in coupling stoichiometry that reduces the probability of successful Orai1–STIM1 coupling. Hence overexpression of TRPC1 in HEK-293 cells may also create an imbalance in the coupling stoichiometry between TRPC1–STIM1 and Orai1–STIM1.

Using an shRNA selectively targeting human TRPC1 [34], we examined the effects of knocking down endogenous TRPC1 in HEK-AC8 cells. The specificity of this TRPC1 shRNA has been documented previously [39], whereby expression of endogenous TRPC1 was significantly reduced, but STIM1 and GAPDH (glyceraldehyde-3-phosphate dehydrogenase) were unaffected by the shRNA. Western blot analysis confirmed a substantial reduction (77%) in TRPC1 protein levels 48 h following transfection compared with control cell lysate (Figure 2A). Specificity of our anti-TRPC1 antibody is shown in Supplementary Figure S1(A), where the antibody detects both endogenous TRPC1 and exogenously expressed HA–TRPC1 proteins. Knockdown of TRPC1 was accompanied by 27±5% reduction in $Ca^{2+}$ entry during Tg-evoked SOCE (Figure 2B) and 43±8% reduction in $Ca^{2+}$ -stimulated cAMP production (Figure 2C). Taken together, these data suggest that TRPC1 contributes to SOCE and can significantly influence AC8 activity. Even so, a significant component of SOCE-induced AC8 activity appears to occur independently of TRPC1, consistent with the AC8 binding partner Orai1 providing the major route of $Ca^{2+}$ entry within the vicinity of AC8 [9,41].

## TRPC1-dependent SOCE-mediated inhibition of AC6 in HSG cells

The contribution of endogenous TRPC1 to SOCE is well-characterized in the HSG cell line, with evidence for Orai1–TRPC1–STIM1 complexes mediating SOCE in lipid raft domains [34,38]. In the present study, we investigated the potential role of TRPC1 in $Ca^{2+}$ -regulated AC activity. RT-PCR analysis of HSG cells was used to ascertain which AC isoforms were likely to be expressed in the salivary gland cell line. Our data revealed an abundance of mRNA for AC6 only (Figure 3A) making the HSG cells ideally suited to studies examining $Ca^{2+}$ -inhibited AC activity. Consistent with our previous work, SOCE in HSG cells was completely inhibited by 100 μM 2APB [34] (Figure 3B). To isolate $Ca^{2+}$ -dependent inhibition of endogenous AC6, the stimulatory effects of the AC activator, 1 μM Fsk on

cAMP production was compared in the presence and absence of 5 mM external $Ca^{2+}$ following store depletion (Figure 3C). All HSG cells were pre-treated with 1 μM Tg in the absence of external $Ca^{2+}$ to deplete the intracellular stores and prime the cell for SOCE following $Ca^{2+}$ re-addition. To enhance the detection of AC6 activity a plasma membrane-targeted cAMP sensor (pm-Epac2-camps) was used to detect cAMP signals close to their site of production [43]. Under control conditions, in the absence of external $Ca^{2+}$, addition of 1 μM Fsk (at 240 s) produced a steady increase in cAMP levels. The stimulatory effects of Fsk were reduced by 60±5% when the AC activator was co-applied with 5 mM external $Ca^{2+}$. These robust inhibitory actions of SOCE on AC6 activity in HSG cells were reversed by treatment with 100 μM 2APB (Figure 3D).

The human TRPC1 selective shRNA used to knockdown expression of endogenous TRPC1 in HEK-293 cells was also very effective in HSG cells (Figure 4A, 75% reduction in protein expression). Knockdown of TRPC1 in the HSG cells was accompanied by ~28% loss of SOCE as detected by theGCaMP2 $Ca^{2+}$ sensor (Figure 4B). The remaining $Ca^{2+}$ entry, representing over 70% of the $Ca^{2+}$ signal, was thought to be mediated by Orai1 and STIM1 acting independently of TRPC1. Even though TRPC1 knockdown only partially reduced SOCE, the associated $Ca^{2+}$ -mediated inhibition of AC6 activity was completely abrogated following TRPC1 knockdown (Figures 4C and 4D) indicating that TRPC1 plays a central role in the $Ca^{2+}$ -dependent inhibition of AC6.

## Effects of TRPC1 compared with Orai1 knockdown on SOCE and $Ca^{2+}$ -stimulated AC8 activity

Data presented so far point towards a clear role for TRPC1 in the $Ca^{2+}$ -dependent regulation of ACs. However, other evidence suggests that TRPC1 can either act independently of Orai1, or that it forms a TRPC1–Orai1–STIM1 assembly to promote SOCE in a variety of cell types including HEK-293 and HSG cells [32,34,35]. To assess whether the actions of TRPC1 on AC8 activity depend on some form of TRPC1 interaction with Orai1, we compared the consequences of the separate knockdown of either TRPC1 or Orai1, with simultaneous knockdown of both channels (Figure 5). The effects of the various knockdowns were compared using the global $Ca^{2+}$ sensor GCaMP2 (Figures 5A and 5B) and cAMP sensor Epac2-camps (Figures 5C and 5D). As before (Figure 2B), knockdown of TRPC1 expression in HEK-AC8 cells was accompanied by a modest, but significant, decrease in both $Ca^{2+}$ entry (Figure 5B, $P < 0.001$) and in SOCE-mediated cAMP production (Figure 5D, $P < 0.05$) when compared with scrambled siRNA control cells.

As reported previously [9] Orai1 knockdown using a selective siRNA resulted in almost complete loss of both $Ca^{2+}$ entry (Figures 5A and 5B) and $Ca^{2+}$ -stimulated AC8 activity (Figures 5C and 5D) compared with scrambled siRNA controls ($P < 0.001$). In the present study, we show that the effects of Orai1 knockdown are significantly greater than the effects seen following knockdown of TRPC1 alone in terms of the reduced SOCE ($P < 0.01$, Figure 5B) and SOCE-induced AC8 activity ($P < 0.01$, Figure 5D). Simultaneous knockdown of both Orai1 and TRPC1 did not decrease SOCE or SOCE-induced AC8 activity any more than that seen following knockdown of Orai1 alone (see Figures 5B and 5D respectively). Therefore Orai1-dependent TRPC1 function underlies the SOCE-dependent regulation of

AC8 in the HEK-AC8 cells. These data further confirm the previous finding that TRPC1 and Orai1 converge on the same $Ca^{2+}$ entry pathway.

## TRPC1-dependent $Ca^{2+}$ entry and cAMP production within the AC8 microdomain

Orai1 knockdown can eliminate almost all SOCE that can be detected globally in HEK-AC8 cells, as shown in Figure 5(B). However, we recently demonstrated that any Orai1 protein that remained after Orai1 siRNA expression could still generate a marked (albeit reduced) $Ca^{2+}$ increase within the AC8 microdomain, giving rise to notable cAMP production in this discrete cellular region [9]. This observation was thought to arise from a direct interaction between AC8 and Orai1 protein that had escaped knockdown by the siRNA, manifesting in a locally restricted signalling event. Using an AC8-targeted version of the $Ca^{2+}$ sensor, GCaMP2-AC8 [12], we confirmed that marked SOCE could still be detected in the AC8 microdomain (Figure 6A) in the face of almost complete loss of the global SOCE signal following Orai1 knockdown (Figure 5A). In contrast, the efficiency of TRPC1 knockdown with respect to $Ca^{2+}$ entry was amplified compared with that seen globally, producing approximately 2-fold greater reduction in $Ca^{2+}$ entry in the AC8 microdomain (Figures 6A and 6B). Nevertheless, this did not result in a greater loss of $Ca^{2+}$ -dependent cAMP production within the AC8 microdomain following TRPC1 knockdown (Figures 6C and 6D). Although SOCE could be clearly detected within the AC8 microdomain following Orai1 knockdown, the $Ca^{2+}$ signal was not decreased further in response to combined TRPC1 and Orai1 knockdown (Figures 6A and 6B). Furthermore, TRPC1 knockdown did not enhance the effects of Orai1 knockdown with respect to cAMP production within the AC8 microdomain (Figures 6C and 6D). This result adds further support to the hypothesis that TRPC1 acts in an Orai1-dependent manner in HEK-AC8 cells and that any contribution to AC8 activity is ultimately also dependent on the presence of Orai1. [The local AC8 domain sensor clearly exaggerates the persisting effects of the Orai1 (in terms of both $Ca^{2+}$ and cAMP) following knockdown with siOrai1 compared with Figure 5, where we are using the global sensors.] Importantly, these data directly reveal local changes in $[Ca^{2+}]_i$ (intracellular $Ca^{2+}$ concentration) that are mediated as a result of store-dependent activation of TRPC1–STIM1 and Orai1–STIM1 channels.

## Evidence of AC8 co-localization with TRPC1 following store depletion

An alternative means of probing the composition of putative TRPC1, Orai1 and AC8 complexes was to examine co-localization of components by confocal TIRF analysis. Following cell stimulation with Tg, TRPC1 co-clusters with both AC8 and STIM1, with areas of co-localization indicated by yellow in control cells (Figure 7A). Even though co-clustering of AC8 and STIM1 was not immediately obvious from the images shown in Figure 7(A), line scan analysis revealed that the puncta for TRPC1, STIM1 andAC8 aggregate at similar sites, as indicated by the coincident peaks in the line scan (Figure 7C). Measurements of fluorescence intensity within selected ROIs showed that the co-clustering of TRPC1 with AC8 and STIM1 increased following stimulation with Tg to promote SOCE, as did the co-clustering of AC8 and STIM1 (Figure 7E). We further investigated the effect of Orai1 knockdown (using siOrai1) on the interactions of TRPC1, STIM1 and AC8. Despite a clear dependence of the contribution of TRPC1 to $Ca^{2+}$ -regulated AC8 activity on Orai1 expression (Figure 6), loss of endogenous Orai1 did not affect the co-clustering of TRPC1,

STIM1 and AC8 (Figures 7B, 7D and 7F). In aggregate, the data show that the co-localization of TRPC1, STIM1 and AC8 after Tg stimulation does not require Orai1. These findings are consistent with our previous observations that, even though TRPC1 clusters with STIM1 in the absence of Orai1, the TRPC1 channel is not functional [39].

## DISCUSSION

The present findings establish a clear contribution from TRPC1 in SOCE-mediated regulation of $Ca^{2+}$ -sensitive ACs. Overexpression or knockdown of Orai1, a recognized pore-forming subunit of CRAC channels [20–22], has been shown previously to have major effects on the amplitude of SOCE events and the accompanying stimulation of AC8 activity [9,41]. Three orthologues of Orai1 have been identified, termed Orai1, Orai2 and Orai3 [44]. Interestingly, activation of arachidonate-regulated $Ca^{2+}$ -selective channels, formed by a hetero-pentameric assembly of three Orai1 subunits and two Orai3 subunits [24], did not result in AC8 regulation [10,13,14]. This latter observation may now be explained by our recent finding that AC8 interacts specifically with a polybasic region of the N-terminal of Orai1 [9]. This latter region is not shown by either Orai2 or Orai3 [44]. The involvement of other potential SOC channel components in AC regulation has not been established apart from evidence that the $Ca^{2+}$ signal arising from DAG (diacylglycerol)-activated TRPC channels (putatively formed from TRPC3–TRPC5–TRPC7 [45]) did not regulate AC8 [13].

Several studies support a role for TRPC1 in SOCE, acting alongside Orai1 and STIM1 [28]. Interestingly, we revealed recently that, although Orai1 knockdown reduced $Ca^{2+}$ -regulated AC8 activity, the effects are less pronounced in the AC8 microdomain, with limited loss of local $Ca^{2+}$ entry and only partial reduction in $Ca^{2+}$ -dependent AC8 activity [9]. One interpretation of this finding was that any remaining Orai1 resided selectively in the AC8 microdomain due to these two proteins directly interacting [9]. However, a second possibility is that other potential SOC channel components, such as TRPC1, might also have influenced the $Ca^{2+}$ and cAMP signals within the cellular microdomain, acting independently of Orai1. In the present study, we reveal that expression levels of TRPC1 have a significant impact on both $Ca^{2+}$ -stimulated and $Ca^{2+}$ -inhibited cAMP production (via AC8 and AC6 respectively), providing the first evidence of any TRPC involvement in AC regulation. Nevertheless, data presented herein point to TRPC1–SOCE effects on AC activity being dependent on Orai1. Overexpression of TRPC1 enhanced AC8 activity only when expressed alongside Orai1 and STIM1 (Figure 1), and simultaneous knockdown of TRPC1 and Orai1 did not inhibit AC8 activity to any greater extent than that seen with knockdown of Orai1 alone (Figure 6). Unlike Orai1 knockdown, the effects of TRPC1 knockdown on $Ca^{2+}$ entry were more pronounced in the AC8 microdomain than seen globally, but this did not result in significantly greater attenuation of the local cAMP signal (compared with that seen globally) (compare Figure 5 with Figure 6). This latter observation suggests that any TRPC1 required for SOCE is likely to preferentially reside alongside Orai1 in the AC8 microdomain, whereas Orai1 is likely to function both inside and outside of the AC8 microdomain largely acting independently of TRPC1 (Figure 8A). The situation in the HSG cells appears somewhat different, with TRPC1 playing a more central role in $Ca^{2+}$ -dependent inhibition of endogenous AC6 activity in this salivary gland cell line (Figure 8B). In the present study, it would seem that all SOCE channels influencing AC6

activity are dependent on TRPC1, with almost complete loss of $Ca^{2+}$ -inhibited AC activity following TRPC1 knockdown (Figure 4). Nevertheless, there is a large capacity for SOCE in HSGs that is apparently independent of TRPC1 expression. We cannot say, based on our data, whether the TRPC1-independent SOCE occurs outside or inside the AC6 microdomain or indeed both.

We now know that Orai1 directly interacts with AC8, and this interaction accounts for the high selectivity of AC8 for this source of $Ca^{2+}$ rise [9]. It remains to be seen whether TRPC1 forms part of the same signalling complex. There is evidence from a range of cell types (including HEK and HSG) of native channels with TRPC1, Orai1 and STIM1 in the same complex [32–35]. Interestingly this interaction is confined to lipid raft regions of the membrane [37,38], the site of $Ca^{2+}$ -regulated AC targeting and function [1]. We have recently proposed that Orai1 and TRPC1 may form separate $Ca^{2+}$ entry channels, both interacting with the ER $Ca^{2+}$ sensor STIM1 [39]. Co-localization of the TRPC1–STIM1 and Orai1–STIM1 channels in sub-plasmalemmal clusters [39] advocates that, even if TRPC1 channels exist as distinct routes of $Ca^{2+}$ entry, TRPC1 could still contribute to $Ca^{2+}$ events within the AC/Orai1 microdomain. Moreover, the dependence of TRPC1 on Orai1 expression to influence AC8 and AC6 activity in the current experiments implies a more integrated action of the two SOC channel components with respect to cAMP production.

Both HEK-293 cells and HSG cells express other TRPC and Orai isoforms (Supplementary Figure S1B). However, SOCE was unaffected by the knockdown of TRPC3, Orai2 and Orai3 using shTRPC3, siOrai2 and siOrai3 respectively (Supplementary Figures S1C and S1D) in HSG cells. Furthermore, knocking down all three Orai1 proteins did not yield further reductions in SOCE when compared with knocking down Orai1 alone in HEK-293 cells (Supplementary Figure S1E). This suggests that Orai1 is the predominant orthologue contributing to SOCE in both cell lines, with minimal contribution from Orai2 and Orai3. The TRPC3 channel, together with TRPC6 and TRPC7 channels, is activated directly by DAG [45]. We had reported previously that DAG-activated $Ca^{2+}$ entry does not stimulate AC8 activity in HEK-293 cells [13]. Furthermore, residues that mediate the interaction of Orai1 with AC8 reside within the polybasic N-terminal region. These residues are specific for Orai1 and are not present on the N-terminus of either Orai2 or Orai3. Therefore it is unlikely that AC8 interacts with either Orai2 or Orai3 [9,44]. Taken together, the data do not support a role for TRPC3, Orai2 and Orai3 in the $Ca^{2+}$ -dependent regulation of ACs. Our studies suggest that in the cell examined here the major effector is likely to be TRPC1 in association with Orai1. However, the possibility exists that other combinations of channels may be efficacious within the AC8 microdomains in other cellular situations.

Data from the present study, using $Ca^{2+}$ sensors targeted to AC8, provide insights into $Ca^{2+}$ dynamics within the AC8 microdomain. Given that we have recently shown that AC8 binds directly to Orai1 via their respective N-termini [9], we can reasonably expect that $Ca^{2+}$ and cAMP will change within the region of the Orai1 channel before $Ca^{2+}$ diffuses out of this domain and other influences dissipate the integrated nature of these signals. In fact, our data are consistent with these suggestions and show rapid increases in both $Ca^{2+}$ and cAMP within the AC8 microdomain that are dependent on Orai1, as well as TRPC1. Furthermore, since ACs are increasingly being shown to be scaffolded to effectors, such as PKA (protein

kinase A), via AKAPs (A-kinase-anchoring proteins) [46], as well as being suggested to bind to a number of additional ion channels [47], these domains may be of profound physiological significance. Thus the tools used in the present study may be useful not only to dissect the components of an AC–$Ca^{2+}$ -signalling complex, but also to permit the dynamics cAMP and $Ca^{2+}$ in such regions to be explored as proposed earlier [12,43].

In conclusion, we have shown that TRPC1 provides an important route of $Ca^{2+}$ entry in HEK-AC8 and HSG cells, influencing $Ca^{2+}$ levels within the microdomain of the ACs and controlling cAMP production. $Ca^{2+}$ inhibition of AC6 appears to be entirely dependent on TRPC1 expression (in HSG cells), whereas TRPC1 regulates only a subset of AC8 molecules (in HEK-293 cells). Future studies may help to elucidate whether the differential dependence of AC6 and AC8 on TRPC1 exists due to distinct properties of the two AC isoforms, differences in the native sub-cellular environment of AC6 compared with AC8, or distinct organization of the SOCE apparatus in the two cell types. However, the implication of a robust regulatory action of TRPC1-dependent $Ca^{2+}$ events on these two widely expressed AC isoforms underlines important downstream functions for TRPC1-dependent SOCE. This is especially relevant in tissues where $Ca^{2+}$ and cAMP signalling are critical for regulation of cell function, such as salivary glands, as well as endothelial and smooth muscle cells and where TRPC1 can play a prominent role in SOCE.

## Supplementary Material

Refer to Web version on PubMed Central for supplementary material.

## Acknowledgments

**FUNDING**

This work was supported by the Wellcome Trust [grant number RG31760 (to D.M.F.C.)] and the NIDCR-DIR (National Institute of Dental and Craniofacial Research Division of Intramural Research) (to I.S.A.).

## Abbreviations

| | |
|---|---|
| **AC** | adenylate cyclase |
| **2APB** | 2-aminoethoxydiphenyl borate |
| **CRAC** | $Ca^{2+}$ release-activated $Ca^{2+}$ |
| **DAG** | diacylglycerol |
| **ER** | endoplasmic reticulum |
| **Fsk** | forskolin |
| **HA** | haemagglutinin |
| **HEK** | human embryonic kidney |
| **HSG** | human submandibular gland |

| | |
|---|---|
| **NFAT** | nuclear factor of activated T-cells |
| **ROI** | region of interest |
| **RT-PCR** | reverse transcription–PCR |
| **SOCE** | store-operated $Ca^{2+}$ entry |
| **STIM1** | stromal interaction molecule 1 |
| **Tg** | thapsigargin |
| **TIRF** | total internal reflection fluorescence |
| **TRPC** | transient receptor potential canonical |

## References


1. Willoughby D, Cooper DMF. Organization and $Ca^{2+}$ regulation of adenylyl cyclases in cAMP microdomains. Physiol. Rev. 2007; 87:965–1010. [PubMed: 17615394]
2. Cali JJ, Zwaagstra JC, Mons N, Cooper DMF, Krupinski J. Type VIII adenylyl cyclase: a $Ca^{2+}$ / calmodulin-stimulated enzyme expressed in discrete regions of rat brain. J. Biol. Chem. 1994; 269:12190–12195. [PubMed: 8163524]
3. Macdougall DA, Wachten S, Ciruela A, Sinz A, Cooper DMF. Separate elements within a single IQ-like motif in adenylyl cyclase type 8 impart $Ca^{2+}$ /calmodulin binding and autoinhibition. J. Biol. Chem. 2009; 284:15573–15588. [PubMed: 19305019]
4. Masada N, Ciruela A, Macdougall DA, Cooper DMF. Distinct mechanisms of regulation by $Ca^{2+}$ / calmodulin of type 1 and 8 adenylyl cyclases support their different physiological roles. J. Biol. Chem. 2009; 284:4451–4463. [PubMed: 19029295]
5. Simpson RE, Ciruela A, Cooper DMF. The role of calmodulin recruitment in $Ca^{2+}$ -stimulation of adenylyl cyclase type 8. J. Biol. Chem. 2006; 281:17379–17389. [PubMed: 16613843]
6. Wu Z, Wong ST, Storm DR. Modification of the calcium and calmodulin sensitivity of the type I adenylyl cyclase by mutagenesis of its calmodulin binding domain. J. Biol. Chem. 1993; 268:23766–23768. [PubMed: 8226907]
7. Guillou J-L, Nakata H, Cooper DMF. Inhibition by calcium of mammalian adenylyl cyclases. J. Biol. Chem. 1999; 274:35539–35545. [PubMed: 10585428]
8. Yoshimura M, Cooper DMF. Cloning and expression of a $Ca^{2+}$ -inhibitable adenylyl cyclase from NCB-20 cells. Proc. Natl. Acad. SciU.SA. 1992; 89:6716–6720.
9. Willoughby D, Everett KL, Halls ML, Pacheco J, Skroblin P, Vaca L, Klussmann E, Cooper DMF. Direct binding between Orai1 and AC8 mediates dynamic interplay between $Ca^{2+}$ and cAMP signaling. Sci. Signal. 2012; 5:ra29. [PubMed: 22494970]
10. Fagan KA, Mons N, Cooper DMF. Dependence of the $Ca^{2+}$ -inhibitable adenylyl cyclase of C6–2B glioma cells on capacitative $Ca^{2+}$ entry. J. Biol. Chem. 1998; 273:9297–9305. [PubMed: 9535924]
11. Willoughby D, Cooper DMF. $Ca^{2+}$ stimulation of adenylyl cyclase generates dynamic oscillations in cyclic AMP. J. Cell Sci. 2006; 119:828–836. [PubMed: 16478784]
12. Willoughby D, Wachten S, Masada N, Cooper DMF. Direct demonstration of discrete $Ca^{2+}$ microdomains associated with different isoforms of adenylyl cyclase. J. Cell Sci. 2010; 123:107–117. [PubMed: 20016071]
13. Martin AC, Cooper DMF. Capacitative and 1-oleyl-2-acetyl-sn-glycerol-activated $Ca^{2+}$ entry distinguished using adenylyl cyclase type 8. Mol. Pharmacol. 2006; 70:769–777. [PubMed: 16723496]

14. Shuttleworth TJ, Thompson JL. Discriminating between capacitative and arachidonate-activated $Ca^{2+}$ entry pathways in HEK293 cells. J. Biol. Chem. 1999; 274:31174–31178. [PubMed: 10531309]
15. Fagan KA, Smith KE, Cooper DMF. Regulation of the $Ca^{2+}$ -inhibitable adenylyl cyclase type VI by capacitative $Ca^{2+}$ entry requires localization in cholesterol-rich domains. J. Biol. Chem. 2000; 275:26530–26537. [PubMed: 10843990]
16. Liou J, Kim ML, Heo WD, Jones JT, Myers JW, Ferrell JE Jr, Meyer T. STIM is a $Ca^{2+}$ sensor essential for $Ca^{2+}$ -store-depletion-triggered $Ca^{2+}$ influx. Curr. Biol. 2005; 15:1235–1241. [PubMed: 16005298]
17. Kawasaki T, Lange I, Feske S. A minimal regulatory domain in the C terminus of STIM1 binds to and activates ORAI1 CRAC channels. Biochem. Biophys. Res. Commun. 2009; 385:49–54. [PubMed: 19433061]
18. Muik M, Fahrner M, Derler I, Schindl R, Bergsmann J, Frischauf I, Groschner K, Romanin C. A cytosolic homomerization and a modulatory domain within STIM1 C terminus determine coupling to ORAI1 channels. J. Biol. Chem. 2009; 284:8421–8426. [PubMed: 19189966]
19. Park CY, Hoover PJ, Mullins FM, Bachhawat P, Covington ED, Raunser S, Walz T, Garcia KC, Dolmetsch RE, Lewis RS. STIM1 clusters and activates CRAC channels via direct binding of a cytosolic domain to Orai1. Cell. 2009; 136:876–890. [PubMed: 19249086]
20. Prakriya M, Feske S, Gwack Y, Srikanth S, Rao A, Hogan PG. Orai1 is an essential pore subunit of the CRAC channel. Nature. 2006; 443:230–233. [PubMed: 16921383]
21. Vig M, Beck A, Billingsley JM, Lis A, Parvez S, Peinelt C, Koomoa DL, Soboloff J, Gill DL, Fleig A, Kinet JP, Penner R. CRACM1 multimers form the ion-selective pore of the CRAC channel. Curr. Biol. 2006; 16:2073–2079. [PubMed: 16978865]
22. Yeromin AV, Zhang SL, Jiang W, Yu Y, Safrina O, Cahalan MD. Molecular identification of the CRAC channel by altered ion selectivity in a mutant of Orai. Nature. 2006; 443:226–229. [PubMed: 16921385]
23. Ji W, Xu P, Li Z, Lu J, Liu L, Zhan Y, Chen Y, Hille B, Xu T, Chen L. Functional stoichiometry of the unitary calcium-release-activated calcium channel. Proc. Natl. Acad. Sci. U.S.A. 2008; 105:13668–13673. [PubMed: 18757751]
24. Mignen O, Thompson JL, Shuttleworth TJ. Orai1 subunit stoichiometry of the mammalian CRAC channel pore. J. Physiol. 2008; 586:419–425. [PubMed: 18006576]
25. Penna A, Demuro A, Yeromin AV, Zhang SL, Safrina O, Parker I, Cahalan MD. The CRAC channel consists of a tetramer formed by Stim-induced dimerization of Orai dimers. Nature. 2008; 456:116–120. [PubMed: 18820677]
26. Luik RM, Wang B, Prakriya M, Wu MM, Lewis RS. Oligomerization of STIM1 couples ER calcium depletion to CRAC channel activation. Nature. 2008; 454:538–542. [PubMed: 18596693]
27. Hardie RC, Minke B. The *trp* gene is essential for a light-activated $Ca^{2+}$ channel in *Drosophila* photoreceptors. Neuron. 1992; 8:643–651. [PubMed: 1314617]
28. Ambudkar IS, Ong HL, Liu X, Bandyopadhyay B, Cheng KT. TRPC1: the link between functionally distinct store-operated calcium channels. Cell Calcium. 2007; 42:213–223. [PubMed: 17350680]
29. Dietrich A, Kalwa H, Storch U, Mederos y Schnitzler M, Salanova B, Pinkenburg O, Dubrovska G, Essin K, Gollasch M, Birnbaumer L, Gudermann T. Pressure-induced and store-operated cation influx in vascular smooth muscle cells is independent of TRPC1. Pflugers Arch. 2007; 455:465–477. [PubMed: 17647013]
30. Varga-Szabo D, Authi KS, Braun A, Bender M, Ambily A, Hassock SR, Gudermann T, Dietrich A, Nieswandt B. Store-operated $Ca^{2+}$ entry in platelets occurs independently of transient receptor potential (TRP) C1. Pflugers Arch. 2008; 457:377–387. [PubMed: 18546016]
31. DeHaven WI, Jones BF, Petranka JG, Smyth JT, Tomita T, Bird GS, Putney JW Jr. TRPC channels function independently of STIM1 and Orai1. J. Physiol. 2009; 587:2275–2298. [PubMed: 19332491]
32. Cheng KT, Liu X, Ong HL, Ambudkar IS. Functional requirement for Orai1 in store-operated TRPC1-STIM1 channels. J. Biol. Chem. 2008; 283:12935–12940. [PubMed: 18326500]

33. Liao Y, Erxleben C, Abramowitz J, Flockerzi V, Zhu MX, Armstrong DL, Birnbaumer L. Functional interactions among Orai1, TRPCs, and STIM1 suggest a STIM-regulated heteromeric Orai/TRPC model for SOCE/Icrac channels. Proc. Natl. Acad. Sci. U.S.A. 2008; 105:2895–2900. [PubMed: 18287061]
34. Ong HL, Cheng KT, Liu X, Bandyopadhyay BC, Paria BC, Soboloff J, Pani B, Gwack Y, Srikanth S, Singh BB, et al. Dynamic assembly of TRPC1/STIM1/Orai1 ternary complex is involved in store operated calcium influx: evidence for similarities in SOC and CRAC channel components. J. Biol. Chem. 2007; 282:9105–9116. [PubMed: 17224452]
35. Kim MS, Zeng W, Yuan JP, Shin DM, Worley PF, Muallem S. Native store-operated $Ca^{2+}$ influx requires the channel function of Orai1 and TRPC1. J. Biol. Chem. 2009; 284:9733–9741. [PubMed: 19228695]
36. Zeng W, Yuan JP, Kim MS, Choi YJ, Huang GN, Worley PF, Muallem S. STIM1 gates TRPC channels, but not Orai1, by electrostatic interaction. Mol. Cell. 2008; 32:439–448. [PubMed: 18995841]
37. Alicia S, Angelica Z, Carlos S, Alfonso S, Vaca L. STIM1 converts TRPC1 from a receptor-operated to a store-operated channel: moving TRPC1 in and out of lipid rafts. Cell Calcium. 2008; 44:479–491. [PubMed: 18420269]
38. Pani B, Ong HL, Liu X, Rauser K, Ambudkar IS, Singh BB. Lipid rafts determine clustering of STIM1 in ER-plasma membrane junctions and regulation of SOCE. J. Biol. Chem. 2008; 283:17333–17340. [PubMed: 18430726]
39. Cheng KT, Liu X, Ong HL, Swaim W, Ambudkar IS. Local $Ca^{2+}$ entry via Orai1 regulates plasma membrane recruitment of TRPC1 and controls cytosolic $Ca^{2+}$ signals required for specific cell functions. PLoS Biol. 2011; 9:e1001025. [PubMed: 21408196]
40. Dobrydneva Y, Abelt CJ, Dovel B, Thadigiri CM, Williams RL, Blackmore PF. 2-Aminoethoxydiphenyl borate as a prototype drug for a group of structurally related calcium channel blockers in human platelets. Mol. Pharmacol. 2006; 69:247–256. [PubMed: 16214957]
41. Martin AC, Willoughby D, Ciruela A, Ayling LJ, Pagano M, Wachten S, Tengholm A, Cooper DMF. Capacitative $Ca^{2+}$ entry via Orai1 and stromal interacting molecule 1 (STIM1) regulates adenylyl cyclase type 8. Mol. Pharmacol. 2009; 75:830–842. [PubMed: 19171672]
42. Soboloff J, Spassova MA, Tang XD, Hewavitharana T, Xu W, Gill DL. Orai1 and STIM reconstitute store-operated calcium channel function. J. Biol. Chem. 2006; 281:20661–20665. [PubMed: 16766533]
43. Wachten S, Masada N, Ayling LJ, Ciruela A, Nikolaev VO, Lohse MJ, Cooper DMF. Distinct pools of cAMP centre on different isoforms of adenylyl cyclase in pituitary-derived GH3B6 cells. J. Cell Sci. 2010; 123:95–106. [PubMed: 20016070]
44. Takahashi Y, Murakami M, Watanabe H, Hasegawa H, Ohba T, Munehisa Y, Nobori K, Ono K, Iijima T, Ito H. Essential role of the N-terminus of murine Orai1 in store-operated $Ca^{2+}$ entry. Biochem. Biophys. Res. Commun. 2007; 356:45–52. [PubMed: 17343823]
45. Hofmann T, Obukhov AG, Schaefer M, Harteneck C, Gudermann T, Schultz G. Direct activation of human TRPC6 and TRPC3 channels by diacylglycerol. Nature. 1999; 397:259–263. [PubMed: 9930701]
46. Dessauer CW. Adenylyl cyclase–A-kinase anchoring protein complexes: the next dimension in cAMP signaling. Mol. Pharmacol. 2009; 76:935–941. [PubMed: 19684092]
47. Zhang M, Patriarchi T, Stein IS, Qian H, Matt L, Nguyen M, Xiang YK, Hell JW. Adenylyl cyclase anchoring by a kinase anchor protein AKAP5 (AKAP79/150) is important for postsynaptic beta-adrenergic signaling. J. Biol. Chem. 2013; 288:17918–17931. [PubMed: 23649627]

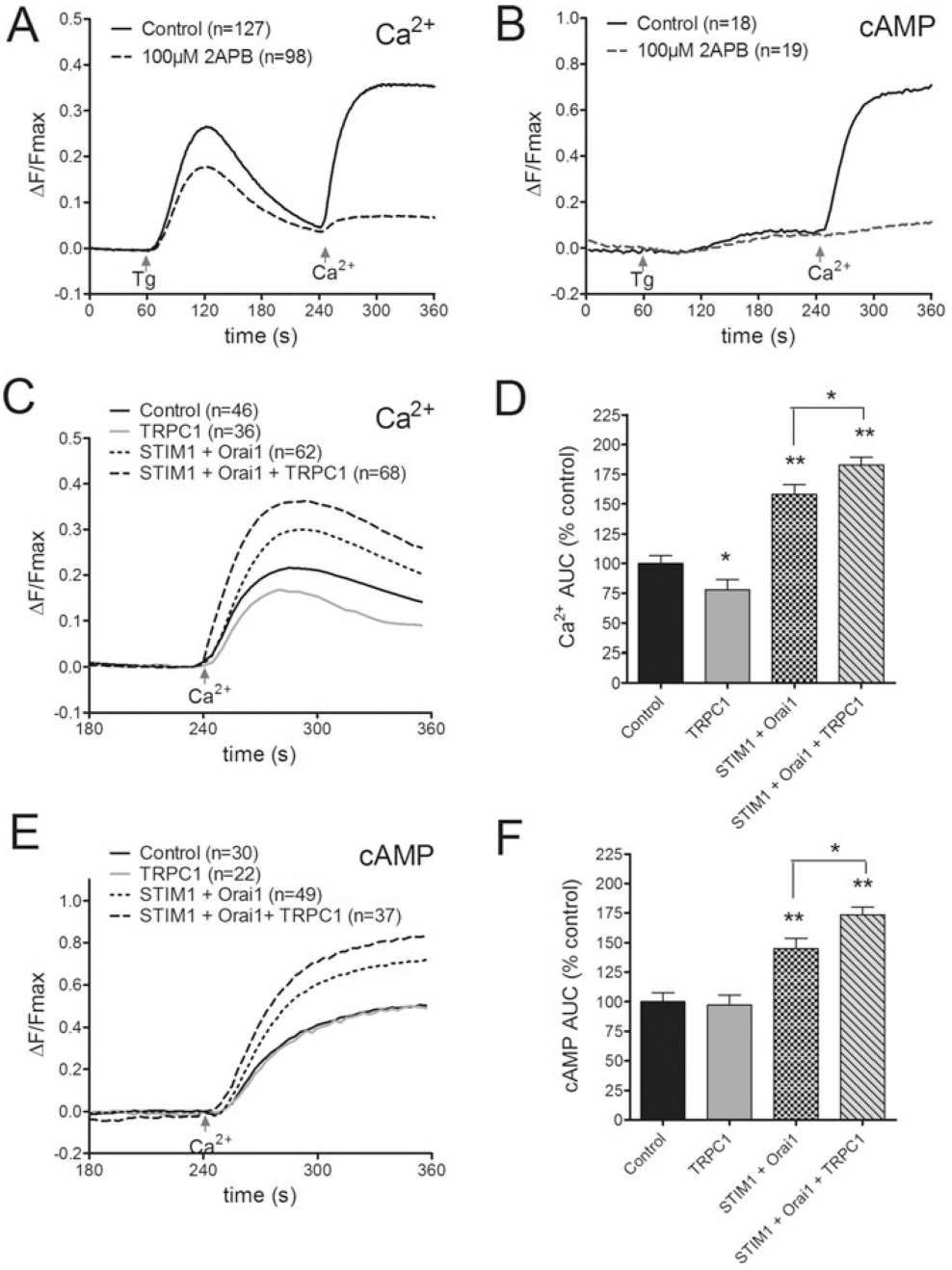


**Figure 1. Effects of STIM1, Orai1 and TRPC1 expression on SOCE-induced AC8 activity in HEK-293 cells**

(**A**) Average single cell fura 2 measurements of HEK-AC8 cells treated at 60 s with 200 nM Tg under zero $Ca^{2+}$ conditions to deplete intracellular $Ca^{2+}$ stores. SOCE was evoked at 240 s by addition of 1 mM external $Ca^{2+}$. The presence of 100 μM 2APB from 60 s onwards blocked SOCE. (**B**) Average data from HEK-AC8 cells expressing the cAMP sensor Epac2-camps show parallel SOCE-stimulated AC8 activity. (**C**) Average effects of HA–TRPC1 overexpression, HA–STIM1 + Myc–Orai1 co-expression, or expression of HA–STIM1 + Myc–Orai1 + HA–TRPC1 on SOCE measured in single HEK-AC8 cells expressing the

GFP-based $Ca^{2+}$ sensor GCaMP2 (**D**) Analysis of data in (**C**) represented as the AUC (area under the curve) between 240 and 360 s. (**E** and **F**) Data from parallel experiments in HEK-AC8 cells expressing Epac2-camps to monitor SOCE-stimulated AC8 activity. The numbers of cells tested are given in parentheses. $*P < 0.05$, $**P < 0.01$ compared with controls unless indicated otherwise. Data were analysed by one-way ANOVA followed by Bonferroni multiple comparisons tests as described in the Experimental section.

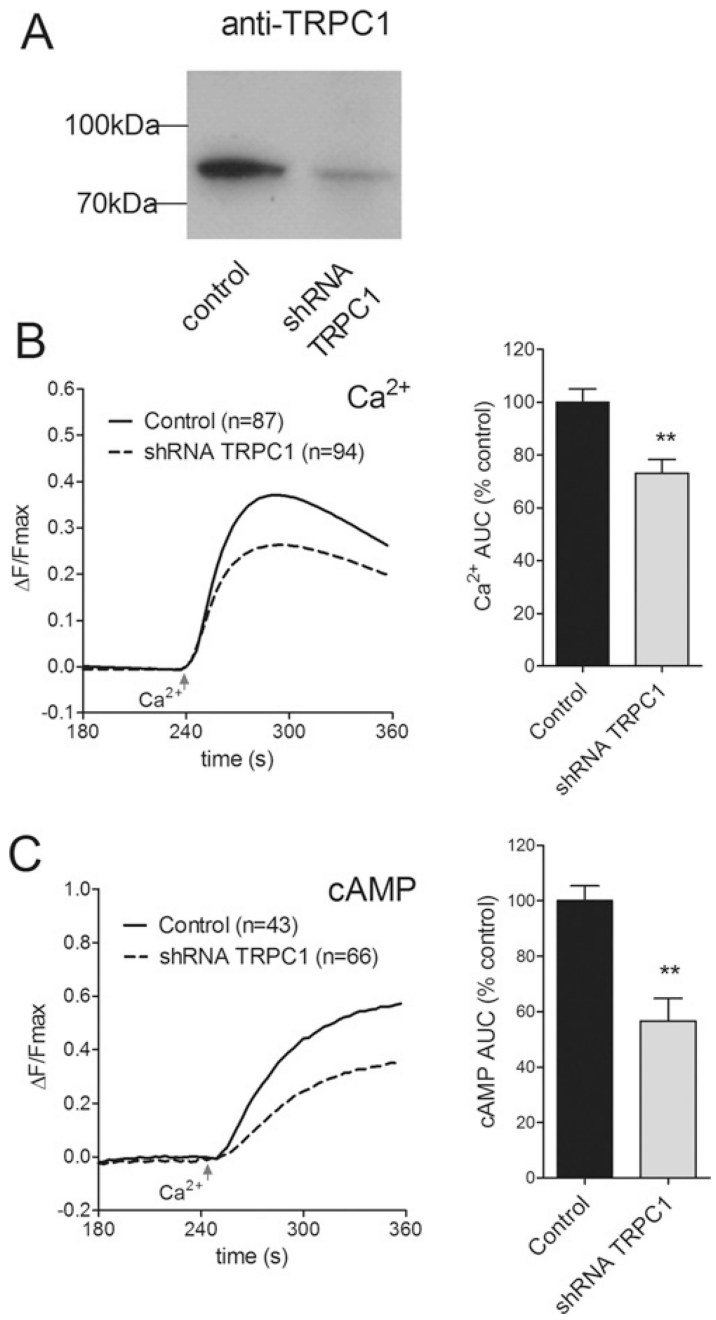


**Figure 2. Effects of TRPC1 knockdown on SOCE-induced AC8 activity**

(**A**) Western blot showing loss of TRPC1 expression in HEK-293 cells ~72 h post-transfection with shRNA selective for human TRPC1. (**B**) Average single cell GCaMP2measurements showing reduced SOCE in HEK-AC8 cells following TRPC1 knockdown. All cells were pre-treated with 200 nM Tg in zero $Ca^{2+}$ conditions to deplete ER $Ca^{2+}$ stores. SOCE was evoked at 240 s by addition of 1 mM external $Ca^{2+}$. (**C**) Data from parallel experiments in HEK-AC8 cells expressing Epac2-camps to monitor SOCE-stimulated AC8 activity. The numbers of cells tested are given in parentheses. $^{**}P < 0.01$ compared with controls.

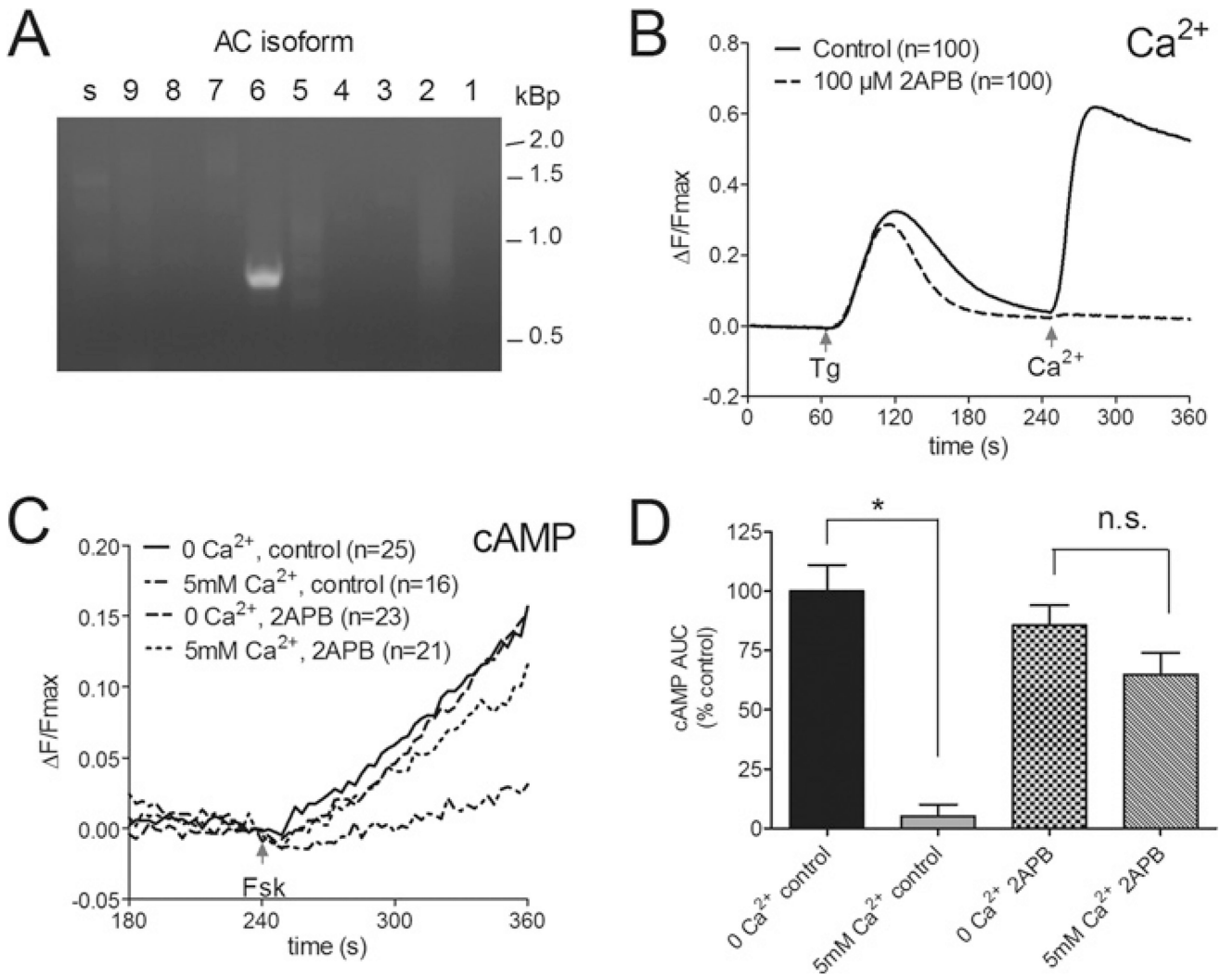


**Figure 3. Evidence of $Ca^{2+}$ -inhibited AC6 activity in HSG cells**

(**A**) RT-PCR analysis of mRNA for all AC isoforms identified AC6 as the major isoform in HSG cells. (**B**) Average single cell fura 2 measurements confirming inhibition of SOCE in HSG cells during treatment with 100 μM 2APB. Cells were pre-treated with 1 μM Tg under zero $Ca^{2+}$ conditions and SOCE was evoked at 240 s by addition of 5 mM external $Ca^{2+}$. (**C**) Average data from HSG cells expressing Epac2-camps to monitor cAMP changes. Fsk (1 μM) was added to cells pre-treated with Tg at 240 s either in the continued absence of $Ca^{2+}$ or presence of 5 mM external $Ca^{2+}$ to induce SOCE. The reduced cAMP production associated with SOCE-inhibited AC6 activity was blocked by treatment with 100 μM 2APB. (**D**) Analysis of data in (**C**) presented as average rate of change of fluorescence ratio ($\Delta F/F_{max}$) per min between 250 and 350 s. The numbers of cells tested are given in parentheses. $^*P < 0.05$. n.s., not significant.

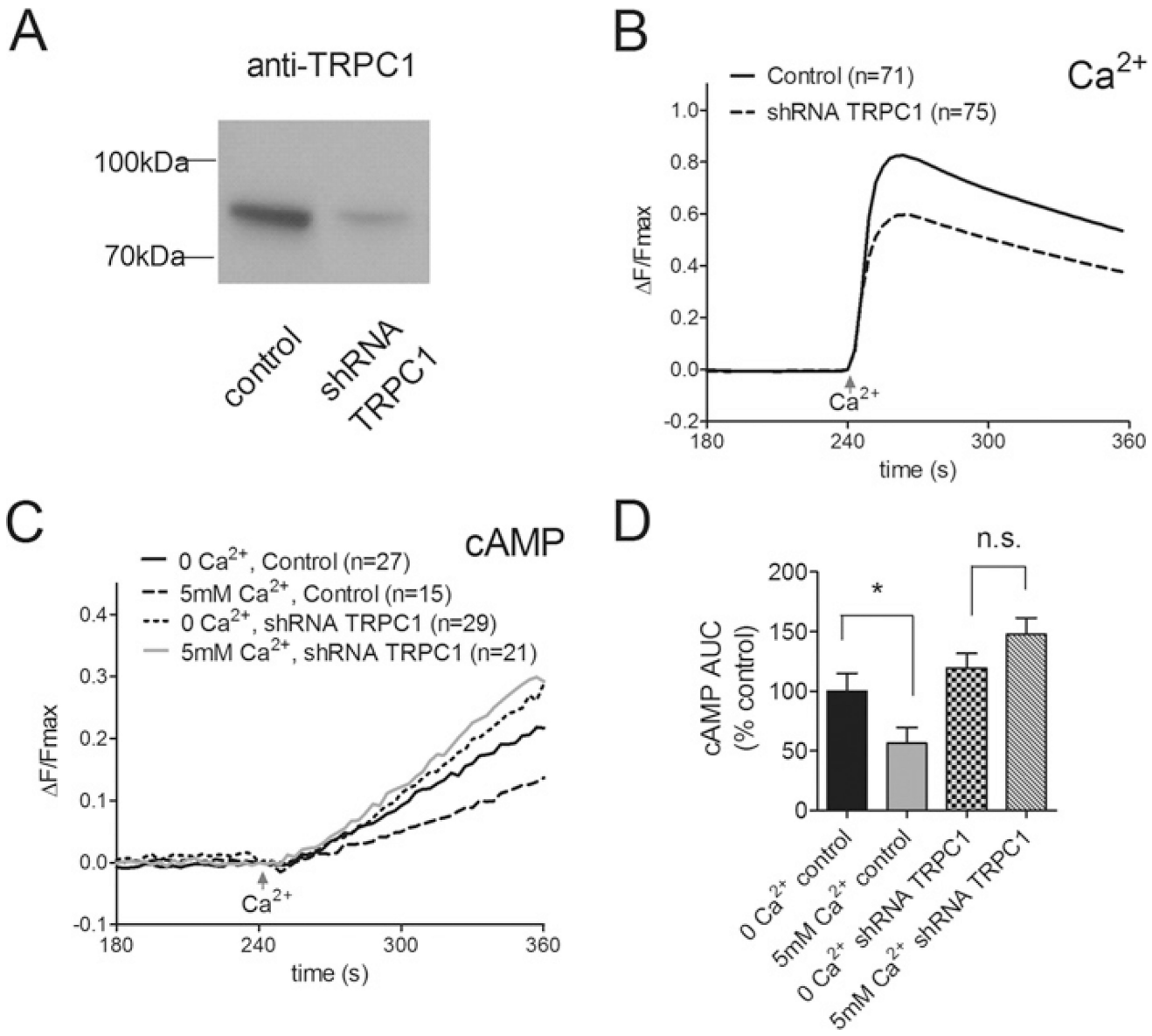


**Figure 4. Effects of TRPC1 knockdown on $Ca^{2+}$ -inhibited AC6 activity in HSG cells**

(**A**) Western blot showing loss of TRPC1 expression in HSG cells ~72 h post-transfection with shRNA selective for human TRPC1. (**B**) Average single cell GCaMP2 measurements showing reduced SOCE in HSG cells following TRPC1 knockdown. All cells were pre-treated with 1 μM Tg and SOCE was evoked at 240 s by addition of 5 mM external $Ca^{2+}$. (**C**) Data from HSG cells expressing Epac2-camps to monitor cAMP changes. Fsk (1 μM) was added to cells pre-treated with Tg at 240 s in the absence or presence of 5 mM external $Ca^{2+}$ to induce SOCE. (**D**) Analysis of data in (**C**) presented as the average rate of change of fluorescence ratio ($\Delta F/F_{max}$) per min between 250 and 350 s, in the absence or presence of external $Ca^{2+}$ without or with TRPC1 knockdown. The reduced cAMP production associated with SOCE-inhibited AC6 activity was reversed following TRPC1 knockdown. The numbers of cells tested are given in parentheses. $*P < 0.05$. n.s., not significant.

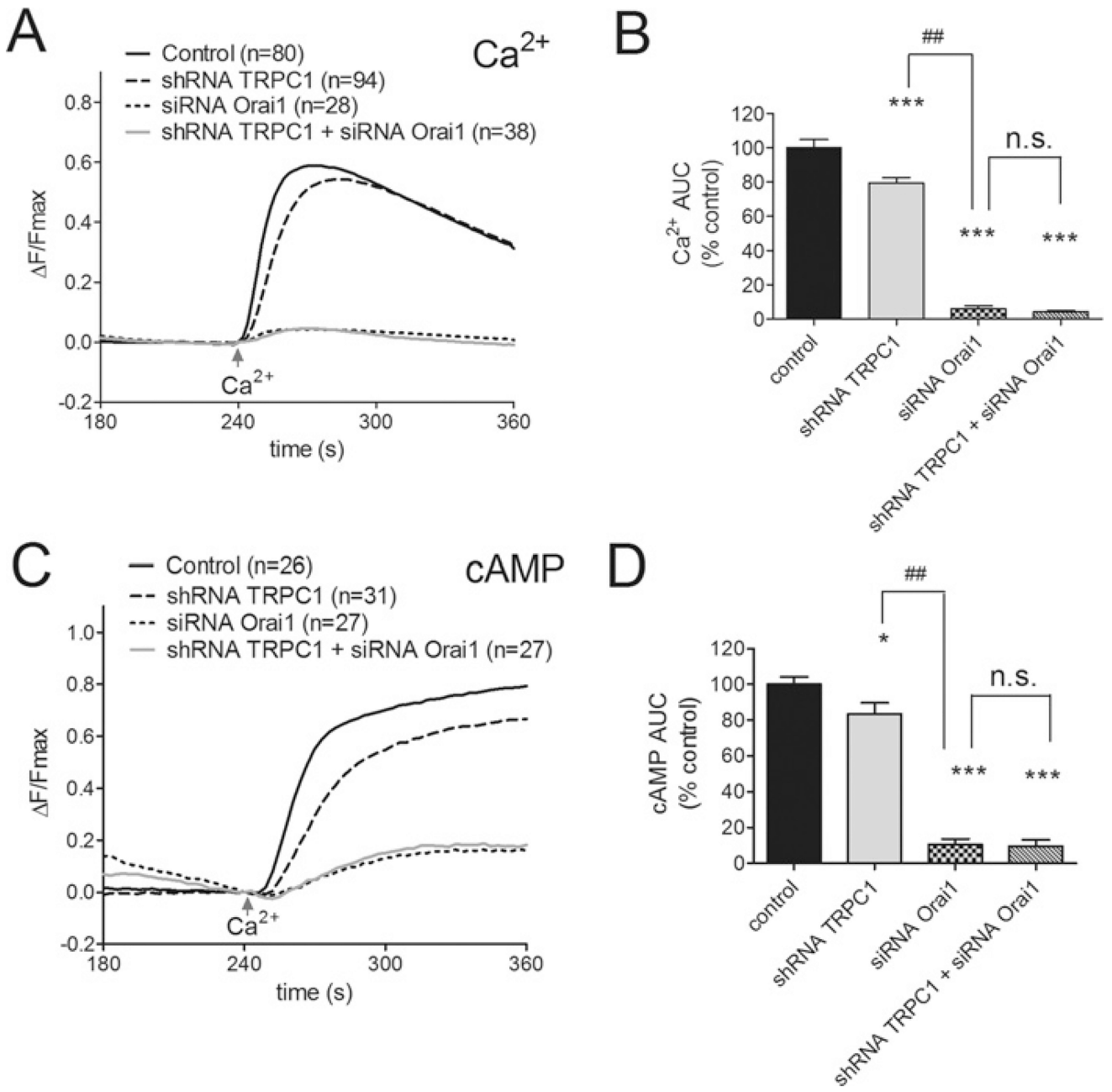


**Figure 5. Comparison of the effects of Orai1 and TRPC1 knockdown on SOCE-induced AC8 activity**

(**A**) The attenuation by Orai1 siRNA and shRNA TRPC1 on SOCE in HEK-AC8 cells expressing GCaMP2 to assess cytosolic $Ca^{2+}$ changes. The effects of Orai1 and TRPC1 knockdown are compared alone and during simultaneous TRPC1 + Orai1 knockdown. All HEK-AC8 cells were pre-treated at 60 s with 200 nM Tg under zero $Ca^{2+}$ conditions and SOCE was evoked by the addition of 1 mM external $Ca^{2+}$ at 240 s. (**B**) The AUC (average area under the curve) GCaMP2 data from (**A**) expressed relative to control SOCE. (**C** and **D**) Data from parallel experiments in HEK-AC8 cells expressing cytosolic Epac2-camps to monitor SOCE-stimulated AC8 activity. The numbers of cells tested are given in

parentheses. *$P < 0.05$, ***$P < 0.001$ compared with controls, $^{\#\#}P < 0.01$ when comparing shRNA TRPC1 and siRNA Orai1 data. n.s., not significant.

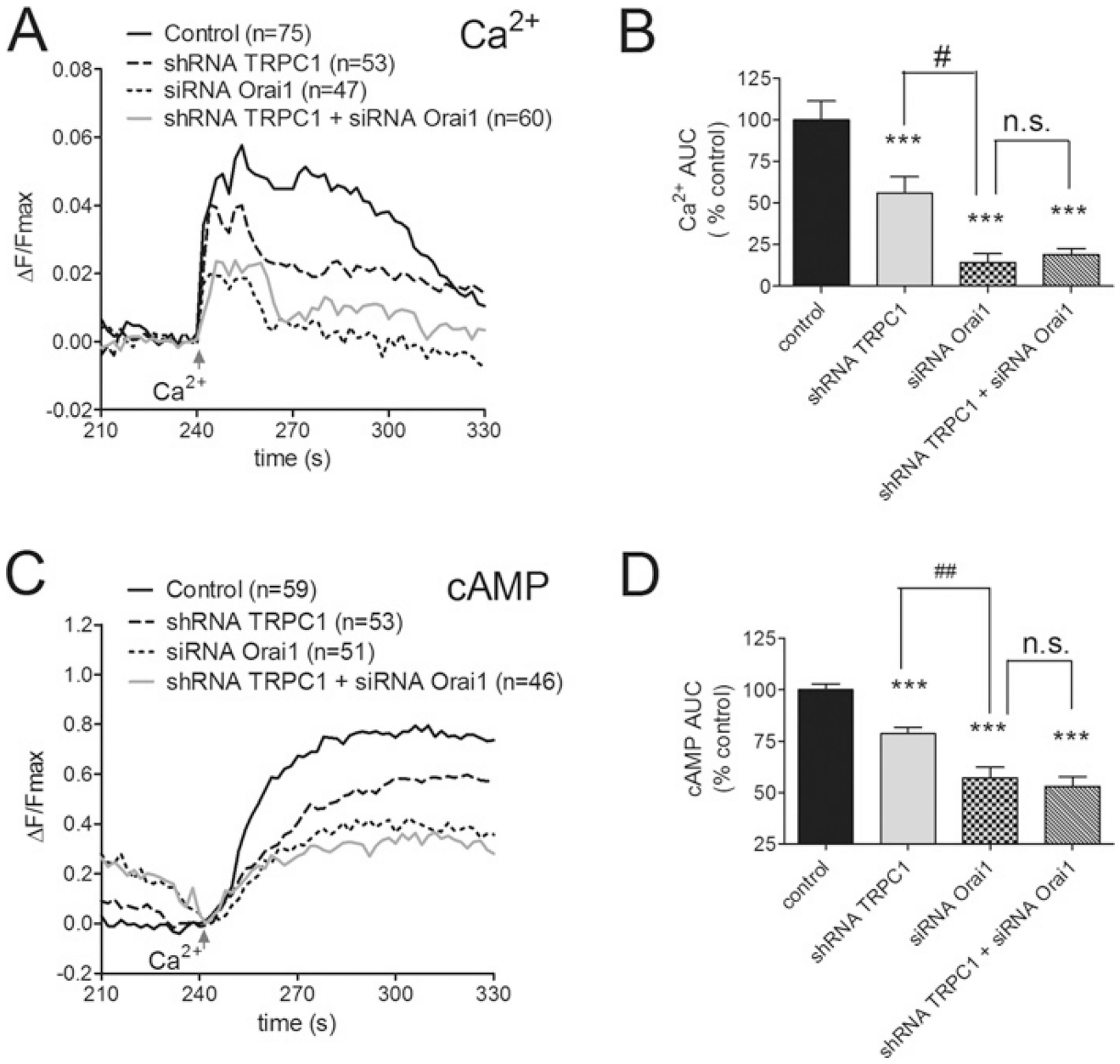


**Figure 6. Effects of Orai1 knockdown and TRPC1 knockdown on SOCE events within the 'AC8 microdomain'**

(**A**) SOCE-associated $Ca^{2+}$ changes within the AC8 microdomain of HEK-AC8 cells monitored using the targeted GCaMP2-AC8 sensor. Traces represent the average $Ca^{2+}$ changes during SOCE under control conditions, or after TRPC1 knockdown alone, Orai1 knockdown alone or simultaneous knockdown of TRPC1 + Orai1. (**B**) AUC (area under the curve) analysis from 240 to 360 s for GCaMP2-AC8 data presented in (**A**) expressed relative to control SOCE data. (**C** and **D**) Data from parallel experiments in HEK-AC8 cells expressing the AC8-targeted cAMP sensor Epac2-camps-AC8 to monitor cAMP changes within the vicinity of AC8. All cells were pre-treated with 200 nM Tg at 60 s and SOCE was evoked by the addition of 1 mM external $Ca^{2+}$ at 240 s. The numbers of cells tested are

shown in parentheses. ***$P < 0.001$ compared with controls, ##$P < 0.01$ when comparing shRNA TRPC1 and siRNA Orai1 data.

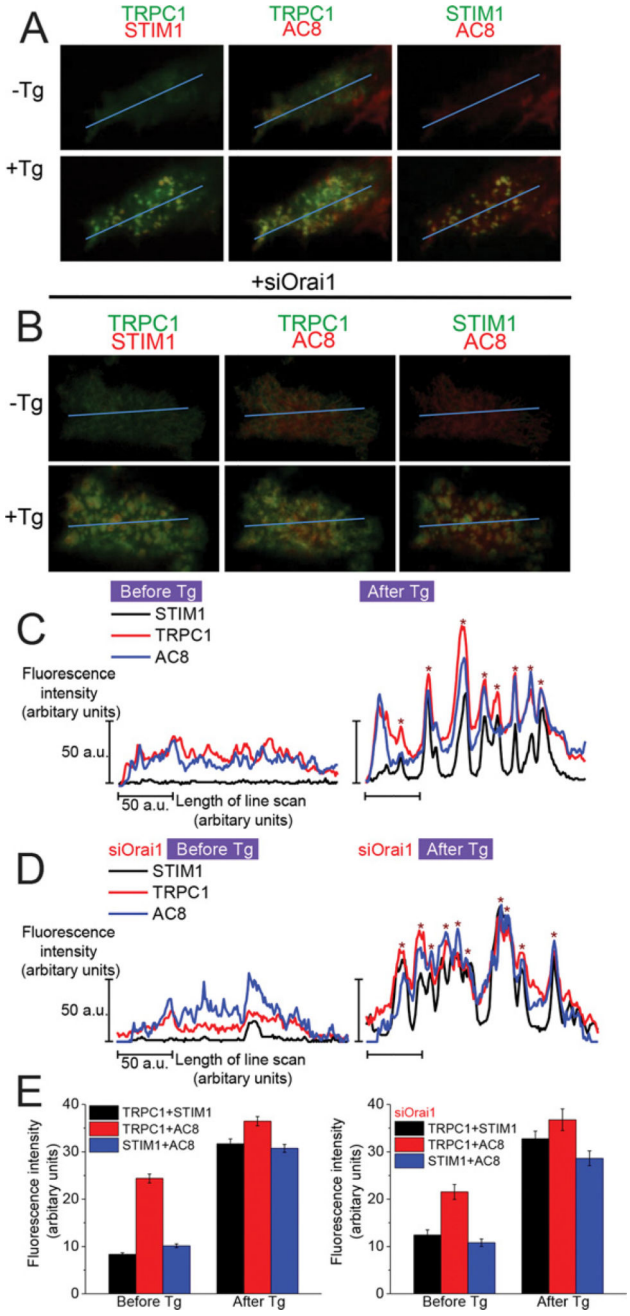


**Figure 7. Co-localization of AC8 with TRPC1 and STIM1 was unaffected by loss of endogenous Orai1**

(**A**) Co-localization of: left-hand panel, TRPC1 (green) and STIM1 (red); middle panel, TRPC1 (green) and AC8 (red); right-hand panel, STIM1 (green) and AC8 (red) in control cells, and (**B**) cells with selective knockdown of Orai1 using siRNA (siOrai1). Areas of co-localization between two proteins are indicated in yellow. (**C**) Line scan measurements showing the fluorescence intensity of AC8, TRPC1 and STIM1 signals along the selected line before and after stimulation with Tg in control cells, and (**D**) siOrai1-treated cells. The coincident intensity peaks of AC8, TRPC1 and STIM1 indicate co-localization of respective puncta for these proteins. Each trace represents data from a single cell and is representative

of ≥five cells, from at least three independent experiments. (**E**) Measurements of ROI fluorescence intensities before and after stimulation with Tg in control cells, and (**F**) siOrai1-treated cells. Data represent the averaged fluorescence intensities of ≥30 ROIs from at least two separate experiments.

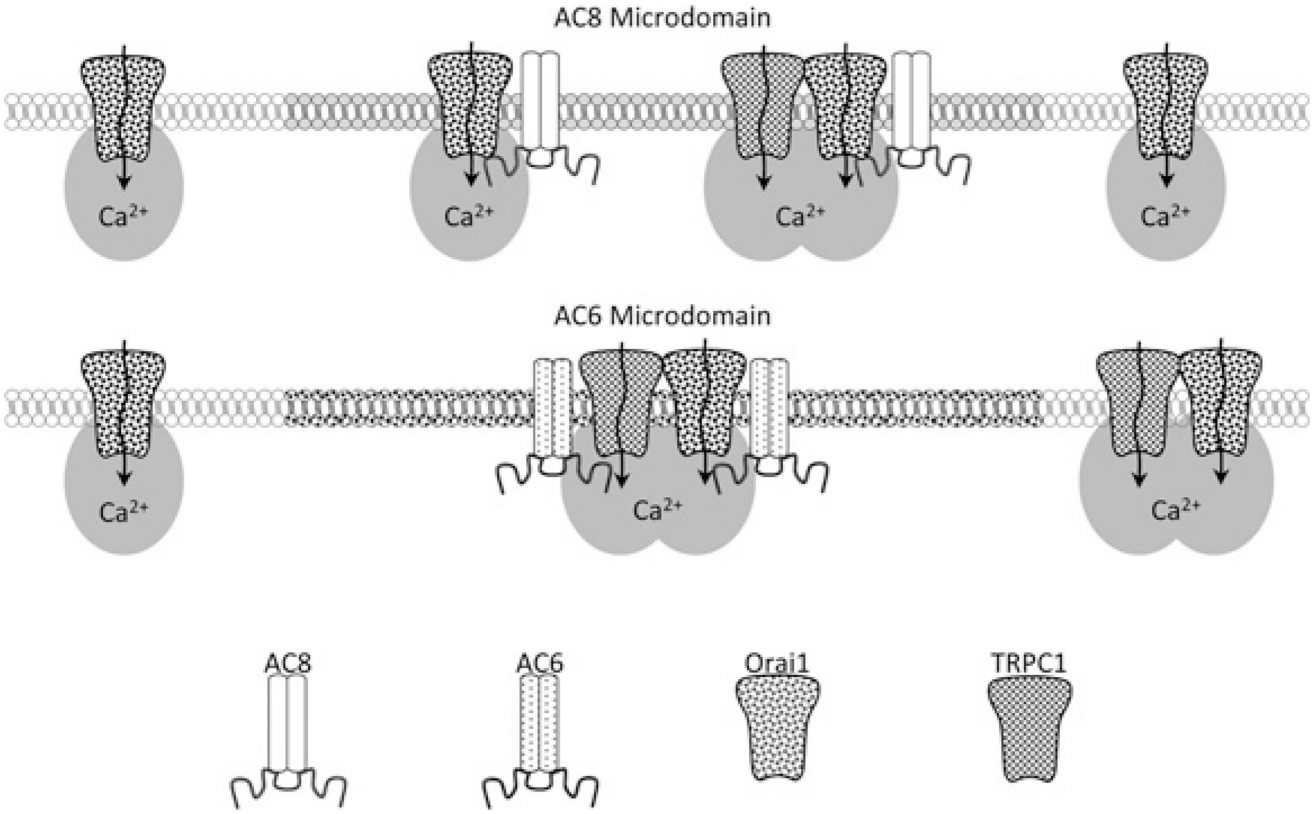


**Figure 8. Proposed model for the contribution of TRPC1 to the regulation of different AC isoforms**

(**A**) In the 'AC8 microdomain' the cyclase is regulated by $Ca^{2+}$ signals arising from Orai1 homomeric SOCE channels, with TRPC1 channels possibly regulating a subset of AC8 molecules. (**B**) cAMP production in the 'AC6 microdomain' is entirely dependent on $Ca^{2+}$ signals generated by activation of TRPC1 channels, although TRPC1-independent SOCE may still occur outside of the 'AC6 microdomain'. Note that in either AC microdomain, TRPC1 function is determined by Orai1 and that the two channels are assembled in a complex.